# Reducible chiral four-body interactions in nuclear matter[1]

N. Kaiser and R. Milkus

Physik-Department T39, Technische Universität München, D-85747 Garching, Germany

*email: nkaiser@ph.tum.de*

**Abstract**

The method of unitary transformations generates five classes of leading-order reducible chiral four-nucleon interactions which involve pion-exchanges and a spin-spin contact-term. Their first-order contributions to the energy per particle of isospin-symmetric nuclear matter and pure neutron matter are evaluated in detail. For most of the closed four-loop diagrams the occurring integrals over four Fermi-spheres can be reduced to easily manageable one- or two-parameter integrals. One observes substantial cancelations among the different contributions arising from 2-ring and 1-ring diagrams. Altogether, the net attraction generated by the chiral four-nucleon interaction does not exceed values of $-1.3\,$MeV for densities $\rho < 2\rho_0$.

## 1 Introduction and summary

According to their modern description and construction in chiral effective field theory, nuclear forces are organized in a hierarchical way [1, 2]. For generic few- and many-body observables the contributions arising from two-nucleon interactions are larger than those from three-nucleon forces, and the latter are again more important than possible corrections due to four-body forces. After a renormalization-group evolution to lower resolution scale such chiral low-momentum interactions exhibit desirable convergence properties in perturbative calculations of many-nucleon systems and infinite nuclear matter [3, 4, 5, 6]. In particular, the inclusion of the leading-order chiral three-nucleon interaction (consisting of contact, $1\pi$-exchange, and $2\pi$-exchange components) is essential in order to achieve saturation of isospin-symmetric nuclear matter in this framework. The calculation of the sub-leading chiral three-nucleon interaction, built up by many pion-loop diagrams etc., has been completed in ref. [7]. By employing chiral two-, three-, and four-nucleon interactions up to order N³LO the equation of state of neutron matter at zero temperature has been studied in detail by the Darmstadt group [8, 9]. A good convergence pattern has been observed for the second and third order particle-particle diagrams with two-nucleon potentials only and when including additionally three-nucleon forces in the form of density-dependent two-body interactions. Moreover, in ref. [9] the N³LO three-body and four-body contributions to the energy per particle of isospin-symmetric nuclear matter have been estimated and large effects from the sub-leading chiral three-nucleon force have been found together with small corrections from the leading-order chiral four-nucleon interactions.

An analytical calculation of chiral four-body interactions in nuclear matter and pure neutron matter has been performed recently in ref. [10]. The long-range four-nucleon interaction is generated by pion-exchanges that are combined by the chiral $4\pi$-vertex (off-shell $\pi\pi$-interaction) or the chiral $NN3\pi$-vertex. The contributions arising from the 2-ring and 1-ring diagrams related to this "irreducible" four-nucleon interaction turned out to be very small, with values below $0.6\,$MeV for densities $\rho < 0.4\,$fm$^{-3}$. However, when including the $\Delta(1232)$-isobar as an explicit degree of freedom and counting the delta-nucleon mass splitting $\Delta = 293\,$MeV as a small scale (comparable to the pion mass $m_\pi$ or the Fermi momentum $k_f$) a new class of leading-order long-range four-nucleon interactions arises. These are mediated by two-fold $\Delta(1232)$-isobar excitation

---

of nucleons and the exchange of three pions. The analytical calculation of the pertinent 3-ring, 2-ring, and 1-ring diagrams at four-loop order has lead to a moderately repulsive contribution of $\bar{E}(\rho_0) = 2.35\,\text{MeV}$ at nuclear matter saturation density $\rho_0 = 0.16\,\text{fm}^{-3}$. However, the curve for $\bar{E}(\rho)$ rises strongly with the density, reaching about 10 times that value at $\rho = 2\rho_0$. In the case of pure neutron matter the same $\Delta(1232)$-induced four-neutron interactions lead to a repulsive contribution that is about half as strong (see Fig. 13 in ref. [10]).

The complete set of leading-order four-nucleon interactions in chiral effective field theory has been constructed by Epelbaum in refs. [11, 12] using the method of unitary transformations. This method allows to project the dynamics of the interacting pion-nucleon system into the purely nucleonic subspace relevant for few-nucleon systems at energies below the pion-production threshold. In addition to the "irreducible" chiral four-nucleon interaction mentioned above, which follows (via the Feynman diagram technique) directly from the vertices of the chiral Lagrangian $\mathcal{L}_{\pi N}^{(1)} + \mathcal{L}_{\pi\pi}^{(2)}$, the method of unitary transformations gives rise to eight classes of "reducible" four-nucleon diagrams. In ref. [12] it is shown that disconnected diagrams always lead to vanishing $4N$-forces and with the kinematically suppressed pion-energies at a Weinberg-Tomozawa $\pi\pi NN$-vertex one obtains that actually three classes (III, VI, and VIII) vanish at leading order. The nonvanishing $4N$-interactions, grouped into the classes I, II, IV, V, and VII, involve multiple pion-exchanges and a spin-spin contact-interaction with coupling constant $C_T$. The associated isoscalar central $NN$-contact term proportional $C_S$ is absent because it drops out of the commutators arising in the construction of the reducible $4N$-interaction. Note that the "irreducible" four-nucleon interaction, which constitutes a part of class II, is called $V^e + V^f$ in ref. [11]. Moreover, one finds that in an anti-symmetrized four-neutron state only the (diagonal) matrix-element of $V^a$ (class I) is nonvanishing and an explicit expression has been given for it in eq.(A14) of ref.[9]. Analogous expressions for the four-nucleon matrix-elements of the other classes have so far not been published.

The purpose present paper is to evaluate analytically the five classes (VII, V, IV, II, I) of reducible chiral four-nucleon interactions ($V^n, V^l, V^k, V^c, V^a$ in the notation of ref. [11]) in isospin-symmetric nuclear matter and pure neutron matter. In order to facilitate a uniform treatment we will first introduce in section 2 a general representation of $4N$-interactions in terms of a product of four (effective) single-nucleon vertices and three "propagator"-factors. The latter will be ordinary pion-propagators, their squares, or just constants. The first-order "Hartree-Fock" contribution to the energy density of nuclear matter is obtained from the connected four-body diagram by closing its four nucleon-lines in all possible ways. The actually occurring chiral vertices have the convenient property that closing any nucleon-line to itself leads to a vanishing spin-trace or isospin-trace. Therefore, one needs to consider here only the closed 2-ring and 1-ring diagrams generated by the reducible chiral $4N$-interactions. These four-loop diagrams are then evaluated individually for the five different classes (in the order VII, V, IV, II, I) in the subsections 2.1 up to 2.5. In most cases the occurring integral over the product of four Fermi spheres of radius $k_f$ can be reduced to an easily manageable one- or two-parameter integral, that depends on the dimensionless ratio $k_f/m_\pi$. The 1-ring diagrams with crossed pion-exchanges related to class II and I allow only for a partial analytical reduction, such that six-parameter integrals remain. The numerical results for the energy per particle $\bar{E}(\rho)$ as a function of the nucleon density $\rho = 2k_f^3/3\pi^2$ are presented and discussed in section 3. We consider two opposite values of the spin-spin contact-coupling, $C_T = 0.22\,\text{fm}^2$ and $C_T = -0.45\,\text{fm}^2$, taken from table I in ref. [9]. One observes substantial cancelations between the contributions from different classes. In particular, the $C_T$-independent classes II and I provide the largest repulsive and attractive contribution, respectively. Altogether, the net attraction generated by the reducible chiral four-nucleon interaction stays above values of $-1.3\,\text{MeV}$ for densities $\rho < 2\rho_0 = 0.32\,\text{fm}^{-3}$. This feature holds for the whole range $|C_T| < 0.5\,\text{fm}^2$ of the spin-spin contact-coupling $C_T$. In the
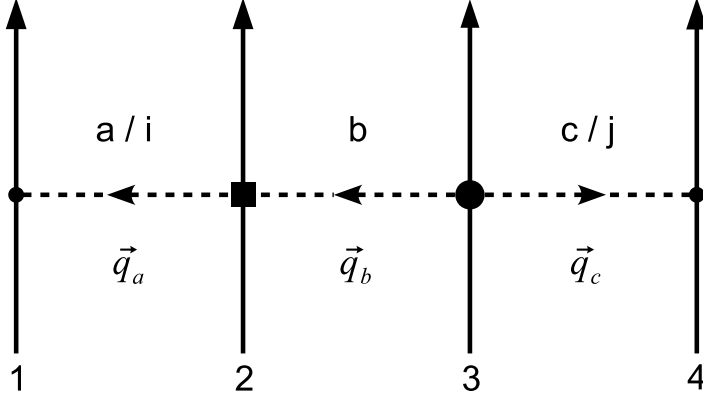
Figure 1: Generic form of the "reducible" chiral 4N-interaction. The square-box and filled circle symbolize effective single-nucleon vertices. The labels $a, b, c$ denote isospin-indices of exchanged pions and $i, j$ denote components of (spin)-vectors.

case of pure neutron matter, where only class I contributes, the result for the energy per particle $\bar{E}_n(\rho_n)$ is determined entirely by a 2-ring diagram, since the three types of 1-ring diagrams compensate each other almost completely. The corresponding attractive energy per particle goes approximately as $\rho_n^{7/3}$ and it reaches a value of about $-2.1\,\text{MeV}$ at $\rho_n = 0.4\,\text{fm}^{-3}$.

In summary one finds that the chiral four-nucleon correlations studied in this work are at least one order of magnitude smaller than those provided by the strongly coupled $\pi N\Delta$-system [10] with its small mass-gap of $293\,\text{MeV}$.

## 2 Diagrammatic calculation of four-body interactions in nuclear matter

In this section we derive analytical expressions for the first-order contributions to the energy per particle of nuclear matter as they arise from the reducible chiral four-nucleon interactions of ref. [12]. In order to facilitate a uniform treatment of the five different classes (VII, V, IV, II, I) we introduce first a generic representation of 4N-interactions in terms of a product of four (effective) single-nucleon vertices and three "propagator"-factors. The latter will be ordinary pion-propagators, their squares, or just constants. Fig. 1 shows the intended generic form of the reducible chiral four-nucleon interaction, represented as an on-shell scattering process $N_1 N_2 N_3 N_4 \to N_1' N_2' N_3' N_4'$. The labels $a, b, c$ denote isospin-indices of exchanged pions and $i, j$ denote components of (spin)-vectors. These vector-indices are introduced by the spin-spin contact-term proportional to $C_T$, and if present, the left and/or right "propagator"-factor is a constant. The momentum transfers $\vec{q}_a = \vec{p}_1' - \vec{p}_1$, $\vec{q}_c = \vec{p}_4' - \vec{p}_4$ and $\vec{q}_b = \vec{p}_2' - \vec{p}_2 + \vec{q}_a = \vec{p}_3 - \vec{p}_3' - \vec{q}_c$ are given by differences of out- and in-going nucleon momenta.

From the generic four-body diagram in Fig. 1 the first-order "Hartree-Fock" contribution to the energy density $\rho\bar{E}(\rho)$ of nuclear matter is obtained by closing the four nucleon-lines in all possible ways. Inspecting the factorized expressions for the five reducible chiral 4N-interactions written in eqs.(1,5,7,10,19) below, one sees that closing any nucleon-line to itself leads to a vanishing spin-trace or isospin-trace. In the case of four neutrons one has either a vanishing spin-trace or a zero from the totally anti-symmetric $\epsilon^{abc}$-tensor, since $\pi^0$-exchange fixed $a = b = 3$. As a consequence of this property, closed 4-ring and 3-ring diagrams vanish trivially and one needs to consider here only the closed 2-ring and 1-ring diagrams generated by the reducible chiral
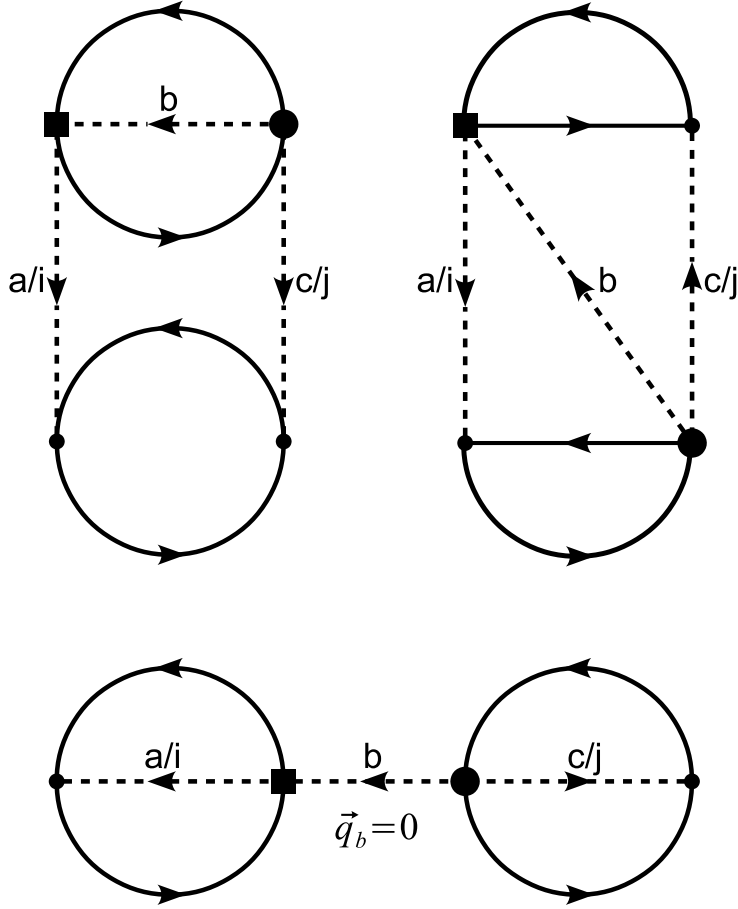
3

Figure 2: Closed two-ring diagrams generated by the reducible chiral 4N-interaction. A symmetry factor $1/2$ occurs, if the square-box and filled-circle vertex are identical. The diagram at the bottom vanishes due to the zero-momentum $\vec{q}_b = \vec{0}$ of the exchanged central pion.

4$N$-interactions.

The three possible 2-ring topologies are shown in Fig. 2. One notices that the diagram at the bottom vanishes due to the zero-momentum $\vec{q}_b = \vec{0}$ of the exchanged central pion. At least one of the adjoined vertices involves $\vec{q}_b$ linearly. Furthermore, the six possible 1-ring topologies are shown in Fig. 3. According to the shape of the dashed (pion) line the diagrams in the first, second, and third row are referred to as U-type, Z-type, and X-type, respectively. Note also that if the square-box and filled-circle vertex represent identical vertices (this happens for class VII and I) a symmetry factor $1/2$ belongs to the 2-ring diagrams and to the Z-type 1-ring diagrams, and obviously identical copies of the U-type and X-type 1-ring diagrams need to be discarded. After these preparations we can now turn to the evaluation of the individual 1-ring and 2-ring diagrams generated by the five classes of reducible chiral 4N-interactions.
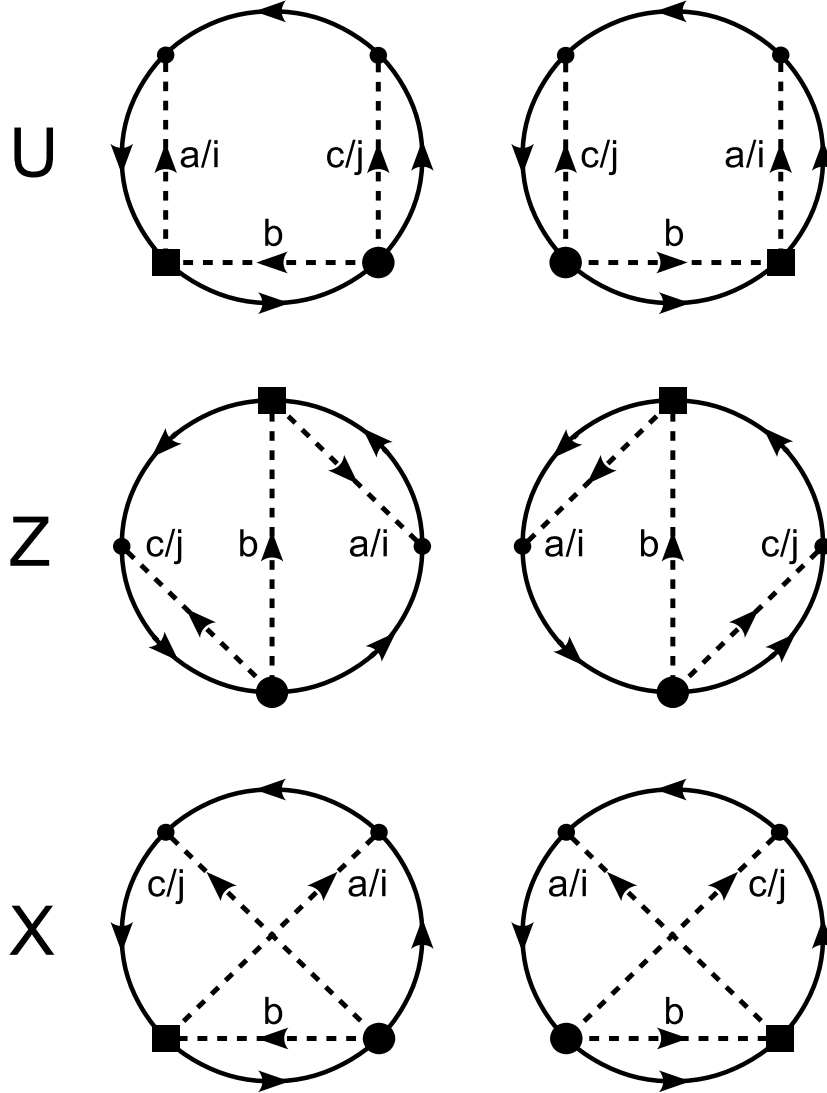
4

Figure 3: Closed one-ring diagrams generated by the reducible chiral 4N-interaction. The diagrams in the first, second, and third row are referred to as U-type, Z-type, and X-type, respectively. A symmetry factor 1/2 belongs to the Z-type diagrams, if the square-box and filled-circle represent identical vertices.

## 2.1 Class VII

We start (in reverse order) with class VII, which is quadratic in the spin-spin contact-coupling $C_T$. The corresponding factorized expression for this chiral 4$N$-interaction reads:

$$V^n = -\frac{C_T^2 g_A^2}{f_\pi^2} \, \sigma_1^i \, (\vec{\sigma}_2 \times \vec{q}_b)^i \, \tau_2^b \, \frac{1}{(m_\pi^2 + \vec{q}_b^2)^2} \, (\vec{\sigma}_3 \times \vec{q}_b)^j \, \tau_3^b \, \sigma_4^j \,. \tag{1}$$

Note that there is an extra factor 2 in comparison to eq.(3.60) in ref. [12] due to the interchange symmetry (12) $\leftrightarrow$ (43) between pairs of nucleons. A straightforward evaluation of the left 2-ring diagram in Fig. 2 gives the following contribution from class VII to the energy per particle of

isospin-symmetric nuclear matter:

$$\bar{E}(\rho) = \frac{3C_T^2 g_A^2 m_\pi^7}{(2\pi^2 u)^3 f_\pi^2} \int_0^u dx \int_0^u dy \, x(u^2 - y^2)(u-x)^2(2u+x)\left\{ -8xy + 6x \right.$$

$$\left. \times \left[ \arctan(2x+2y) - \arctan(2x-2y) \right] + (2x^2 - 2y^2 - 1)\ln\frac{1+4(x+y)^2}{1+4(x-y)^2} \right\}, \quad (2)$$

with the dimensionless variable $u = k_f/m_\pi$. The nucleon density $\rho = 2k_f^3/3\pi^2$ is related to the Fermi momentum $k_f$ in the usual way. In order to arrive at a double-integral representation we have used the reduction formula:

$$\int_0^u dp \int_{-1}^1 dz \, p^2 F\left(pz + \sqrt{u^2 - p^2(1-z^2)}\right) = \int_0^u dy \, (u^2 - y^2) F(2y), \quad (3)$$

to eliminate a complicated angular integral, and a master formula for integrating $F(|\vec{p}_1 - \vec{p}_2|)$ over two Fermi spheres $|\vec{p}_{1,2}| < k_f$. The latter introduces the weighting-function $x^2(u-x)^2(2u+x)$. Actually, there exists an analytical solution of the double-integral in eq.(2), namely:

$$\bar{E}(\rho) = \frac{C_T^2 g_A^2 m_\pi^7}{140\pi^6 f_\pi^2}\left\{ \frac{u}{160} - \frac{31u^3}{48} + \frac{229u^5}{20} - \frac{179u^7}{10} \right.$$

$$+ \left( \frac{3}{16} + \frac{343u^2}{40} + 20u^4 - \frac{142u^6}{3} \right)\arctan 2u$$

$$+ \left( \frac{176u^6}{3} - 10u^4 - \frac{343u^2}{80} - \frac{3}{32} \right)\arctan 4u$$

$$+ \left( 28u^5 - \frac{32u^7}{5} + \frac{35u^3}{8} - \frac{7u}{8} - \frac{5}{128u} - \frac{1}{3840u^3} \right)\ln(1+4u^2)$$

$$+ \left( \frac{32u^7}{5} - 28u^5 - \frac{35u^3}{8} + \frac{7u}{32} + \frac{5}{512u} + \frac{1}{15360u^3} \right)\ln(1+16u^2) \right\}. \quad (4)$$

Note that in the chiral limit $m_\pi \to 0$ only a term $u^7(128\ln 2 - 179)/10 = -9.0277\,u^7$ remains. Let us also comment on the features of the other diagrams for class VII: The right 2-ring diagram in Fig 2 leads to a vanishing isospin-trace in symmetric nuclear matter, whereas in pure neutron matter the left and right 2-ring diagram cancel each other. The U-type and Z-type 1-ring diagrams in Fig. 3 cancel each other after taking the spin-trace, and the X-type 1-ring diagram leads to a vanishing spin-trace by itself.

## 2.2 Class V

Next we come to class V, which is induced by the Weinberg-Tomozawa $\pi\pi NN$-vertex in combination with the spin-spin contact-coupling $C_T$. The corresponding factorized expression for this chiral $4N$-interaction reads [12]:

$$V^l = \frac{C_T g_A^2}{8f_\pi^4} \vec{\sigma}_1 \cdot \vec{q}_a \, \tau_1^a \, \frac{1}{m_\pi^2 + \vec{q}_a^2} \, \epsilon^{abc} \, \tau_2^c \, \frac{1}{m_\pi^2 + \vec{q}_b^2} \, (\vec{\sigma}_3 \times \vec{q}_b)^j \, \tau_3^b \, \sigma_4^j, \quad (5)$$

and it obviously vanishes for four neutrons, where only $\pi^0$-exchange is possible ($\epsilon^{33c} = 0$). The evaluation of the X-type 1-ring diagram in Fig. 3 gives the following contribution from class V to

6

the energy per particle of isospin-symmetric nuclear matter:

$$
\begin{aligned}
\bar{E}(\rho) &= \frac{3C_T g_A^2 m_\pi^7}{(2\pi)^6 f_\pi^4 u^3} \int_0^u dx \int_0^u dy \, \frac{x(u^2 - y^2)}{1 + 4x^2}(u - x)^2(2u + x)\Bigg\{ -4xy \\
&\quad \times (1 + 4x^2 + 4y^2) + \frac{1}{4}\left[1 + 4(x + y)^2\right]\left[1 + 4(x - y)^2\right]\ln\frac{1 + 4(x + y)^2}{1 + 4(x - y)^2}\Bigg\}.
\end{aligned} \tag{6}
$$

Note that the integral $\int_0^u dy \ldots$ could be solved in terms of elementary functions $(\ln, \arctan)$, but we refrain from presenting this rather lengthy expression. The same applies to the subsequent results given in eqs.(8,9,11,20,21). Concerning the other diagrams for class V, one finds that both 2-ring diagrams in Fig. 2 lead to a vanishing spin- and isospin-trace. Moreover, the U-type and Z-type 1-ring diagrams in Fig. 3 cancel each other after taking the spin-trace.

## 2.3  Class IV

Next we come to class VI, which is induced by the spin-spin contact-coupling $C_T$ in combination with a "contraction" of two ordinary $\pi N$-vertices. The corresponding factorized expression for this chiral $4N$-interaction reads [12]:

$$
V^k = -\frac{C_T g_A^4}{4f_\pi^4}\, \vec{\sigma}_1 \cdot \vec{q}_a\, \tau_1^a\, \frac{1}{m_\pi^2 + \vec{q}_a^2}\left[\epsilon^{abc}\, \tau_2^c\, \vec{q}_a \cdot \vec{q}_b + \delta^{ab}\, \vec{\sigma}_2 \cdot (\vec{q}_a \times \vec{q}_b)\right]\frac{1}{(m_\pi^2 + \vec{q}_b^2)^2}\,(\vec{\sigma}_3 \times \vec{q}_b)^j\, \tau_3^b\, \sigma_4^j. \tag{7}
$$

Whereas the left 2-ring diagram has a vanishing isospin-trace, one obtains from the right 2-ring diagram the following contribution to the energy per particle of isospin-symmetric nuclear matter:

$$
\begin{aligned}
\bar{E}(\rho) &= \frac{3C_T g_A^4 m_\pi^7}{16\pi^6 f_\pi^4 u^3}\int_0^u dx \int_0^u dy\, \frac{x(u^2 - y^2)}{1 + 4x^2}(u - x)^2(2u + x) \\
&\quad \times \Bigg\{ xy(1 - 12x^2 + 4y^2) + 8x^3\left[\arctan(2x + 2y) - \arctan(2x - 2y)\right] \\
&\quad + \left(3x^4 - \frac{3x^2 + y^2}{2} - 2x^2 y^2 - y^4 - \frac{1}{16}\right)\ln\frac{1 + 4(x + y)^2}{1 + 4(x - y)^2}\Bigg\}.
\end{aligned} \tag{8}
$$

By rewriting the spin- and isospin-factors as a product of two anti-commutators one finds that the U-type and Z-type 1-ring diagrams add to zero. On the other hand, the X-type 1-ring diagrams in Fig. 3 give a contribution to $\bar{E}(\rho)$ of the form:

$$
\begin{aligned}
\bar{E}(\rho) &= \frac{3C_T g_A^4 m_\pi^7}{16\pi^6 f_\pi^4 u^3}\int_0^u dx \int_0^u dy\, \frac{x(u^2 - y^2)}{1 + 4x^2}(u - x)^2(2u + x) \\
&\quad \times \Bigg\{ 2xy(1 + 4x^2 + 4y^2) + 8x^3\left[\arctan(2x - 2y) - \arctan(2x + 2y)\right] \\
&\quad + \left(x^2 - 2x^4 + 4x^2 y^2 - y^2 - 2y^4 - \frac{1}{8}\right)\ln\frac{1 + 4(x + y)^2}{1 + 4(x - y)^2}\Bigg\}.
\end{aligned} \tag{9}
$$

In the case of pure neutron matter the left and right 2-ring diagram cancel each other, likewise do this the U-type and Z-type 1-ring diagrams, and the X-type 1-ring diagrams vanish by themselves (because for four neutrons the $\epsilon^{abc}$-term in $V^k$ is absent).

## 2.4  Class II

Next we come to class II, which is induced by the Weinberg-Tomozawa $\pi\pi NN$-vertex in combination with the "contraction" of two ordinary $\pi N$-vertices. The corresponding factorized expression

for this $3\pi$-exchange $4N$-interaction reads [12]:

$$V^c = -\frac{g_A^4}{32 f_\pi^6} \, \vec{\sigma}_1 \cdot \vec{q}_a \, \tau_1^a \, \frac{1}{m_\pi^2 + \vec{q}_a^2} \, \epsilon^{abd} \, \tau_2^d \, \frac{1}{m_\pi^2 + \vec{q}_b^2}$$

$$\times \left[ \epsilon^{bce} \, \tau_3^e \, \vec{q}_b \cdot \vec{q}_c + \delta^{bc} \, \vec{\sigma}_3 \cdot (\vec{q}_b \times \vec{q}_c) \right] \frac{1}{m_\pi^2 + \vec{q}_c^2} \, \vec{\sigma}_4 \cdot \vec{q}_c \, \tau_4^c \,, \tag{10}$$

and it obviously vanishes for four neutrons, since $\epsilon^{33d} = 0$. The evaluation of the left 2-ring diagram in Fig. 2 gives the following contribution to the energy per particle of isospin-symmetric nuclear matter:

$$\bar{E}(\rho) = \frac{3 g_A^4 m_\pi^7}{(2\pi f_\pi)^6 u^3} \int_0^u dx \int_0^u dy \, \frac{x^3 (u^2 - y^2)}{(1 + 4x^2)^2} (u-x)^2 (2u+x) \left\{ 4xy \right.$$

$$\left. \times (1 + 4x^2 + 4y^2) - \frac{1}{4} \left[ 1 + 4(x+y)^2 \right] \left[ 1 + 4(x-y)^2 \right] \ln \frac{1 + 4(x+y)^2}{1 + 4(x-y)^2} \right\}, \tag{11}$$

whereas the right 2-ring diagram produces a vanishing spin-trace. In the case of the U-type 1-ring diagrams in Fig. 3, three (out of four) Fermi sphere integrals over the pion-propagators and momentum-dependent interactions factorize by making use of tensor-contractions. For this reason one can represent the corresponding contribution to $\bar{E}(\rho)$ as a one-parameter integral of the form:

$$\bar{E}(\rho) = -\frac{3 g_A^4 m_\pi^7}{4(4\pi f_\pi)^6 u^3} \int_0^u dx \, \frac{G_V^2(x)}{x} \left[ 2 G_S(x) + G_T(x) \right]. \tag{12}$$

Here, we have introduced the auxiliary functions:

$$G_V(x) = u(1 + u^2 + x^2) - \frac{1}{4x} \left[ 1 + (u+x)^2 \right] \left[ 1 + (u-x)^2 \right] \ln \frac{1 + (u+x)^2}{1 + (u-x)^2}, \tag{13}$$

$$G_S(x) = \frac{4ux}{3}(2u^2 - 3) + 4x \left[ \arctan(u+x) + \arctan(u-x) \right]$$

$$+ (x^2 - u^2 - 1) \ln \frac{1 + (u+x)^2}{1 + (u-x)^2}, \tag{14}$$

$$G_T(x) = \frac{ux}{6}(8u^2 + 3x^2) - \frac{u}{2x}(1 + u^2)^2 + \frac{1}{8} \left[ \frac{(1+u^2)^3}{x^2} \right.$$

$$\left. - x^4 + (1 - 3u^2)(1 + u^2 - x^2) \right] \ln \frac{1 + (u+x)^2}{1 + (u-x)^2}, \tag{15}$$

defined by vectorial and tensorial Fermi sphere integrals over a pion-propagator (see also eq.(A.1) in ref. [10]). In the case of the Z-type 1-ring diagrams in Fig. 3, the two Fermi sphere integrals over the pion-propagators associated to the short pion-lines factorize via tensors. For the remaining two Fermi sphere integrals the angular part can be carried out, and in this procedure the third pion-propagator introduces the logarithmic function:

$$\mathbf{L} = \ln \frac{1 + (x+y)^2}{1 + (x-y)^2}. \tag{16}$$

Putting all pieces together, one obtains the following double-integral representation for the contribution of the Z-type 1-ring diagrams from class II to the energy per particle of nuclear matter:

$$\bar{E}(\rho) = \frac{3 g_A^4 m_\pi^7}{(4\pi f_\pi)^6 u^3} \int_0^u dx \int_0^u dy \, G_V(x) \left\{ G_S(y) \left[ 2y + \frac{\mathbf{L}}{2x}(x^2 - y^2 - 1) \right] \right.$$

$$\left. + \frac{G_T(y)}{4y} \left[ y^2 - 3x^2 - 3 + \frac{\mathbf{L}}{4xy} \left( 3(1 + x^2)^2 + 2y^2 - 2x^2 y^2 - y^4 \right) \right] \right\}. \tag{17}$$

In the case of the X-type 1-ring diagrams in Fig. 3 the assignment of momenta to the virtual pions is now such that the previous factorization approach does not work anymore. Only the Fermi sphere integral associated to the nucleon-line between the square-box and filled-circle vertex can be performed analytically. Hence, the contribution of the X-type 1-ring diagrams from class II to the energy per particle of nuclear matter result in the form:

$$\bar{E}(\rho) = \frac{9g_A^4 m_\pi^7}{(4\pi f_\pi)^6 u^3} \int_{|\vec{p}_j|<u} \frac{d^3 p_1\, d^3 p_2\, d^3 p_3}{(2\pi)^3} \frac{G_V(|\vec{\eta}|)}{(1+\vec{q}_1^{\,2})(1+\vec{q}_2^{\,2})\,\vec{\eta}^{\,2}} \left[(\vec{q}_1 - \vec{q}_2)\cdot \vec{q}_2\right] (\vec{q}_1 \cdot \vec{\eta}), \qquad (18)$$

with $\vec{q}_1 = \vec{p}_1 - \vec{p}_3$, $\vec{q}_2 = \vec{p}_2 - \vec{p}_3$ and $\vec{\eta} = \vec{p}_1 + \vec{p}_2 - \vec{p}_3$, where all momentum-vectors have been divided by the pion mass $m_\pi$. Note that due to rotational invariance it is sufficient to parametrize the nine-dimensional integral in eq.(18) by three radii $(0 < p_{1,2,3} < u)$, two directional cosines $(-1 < z_{1,2} < 1)$, and one azimuthal angle $(0 < \varphi < 2\pi)$.

## 2.5   Class I

Finally we come to class I, which is induced by a pair of "contractions" of two ordinary $\pi N$-vertices. The corresponding factorized expression for this $3\pi$-exchange $4N$-interaction reads:

$$\begin{aligned}
V^a &= \frac{g_A^6}{16 f_\pi^6} \vec{\sigma}_1 \cdot \vec{q}_a\, \tau_1^a \frac{1}{m_\pi^2 + \vec{q}_a^{\,2}} \left[\epsilon^{abd}\, \tau_2^d\, \vec{q}_a \cdot \vec{q}_b + \delta^{ab}\, \vec{\sigma}_2 \cdot (\vec{q}_a \times \vec{q}_b)\right] \\
&\quad \times \frac{1}{(m_\pi^2 + \vec{q}_b^{\,2})^2} \left[\epsilon^{bce}\, \tau_3^e\, \vec{q}_b \cdot \vec{q}_c + \delta^{bc}\, \vec{\sigma}_3 \cdot (\vec{q}_b \times \vec{q}_c)\right] \frac{1}{m_\pi^2 + \vec{q}_c^{\,2}} \vec{\sigma}_4 \cdot \vec{q}_c\, \tau_4^c, \qquad (19)
\end{aligned}$$

Note that there is again an extra factor 2 in comparison to eq.(3.33) in ref. [12] due to the interchange symmetry (12) $\leftrightarrow$ (43) between pairs of nucleons. The evaluation of the left 2-ring diagram in Fig. 2 gives the following contributions to the energy per particle of isospin-symmetric nuclear matter:

$$\begin{aligned}
\bar{E}(\rho) &= \frac{3g_A^6 m_\pi^7}{(2\pi f_\pi)^6 u^3} \int_0^u dx \int_0^u dy\, \frac{x^3(u^2 - y^2)}{(1+4x^2)^2}(u-x)^2(2u+x) \\
&\quad \times \Bigg\{ -2xy(1 + 20x^2 + 4y^2) + 32x^3 \big[\arctan(2x+2y) - \arctan(2x-2y)\big] \\
&\quad + \Big(10x^4 - 5x^2 + y^2 - 12x^2 y^2 + 2y^4 + \frac{1}{8}\Big) \ln \frac{1+4(x+y)^2}{1+4(x-y)^2} \Bigg\}, \qquad (20)
\end{aligned}$$

and to the energy per particle of pure neutron matter:

$$\begin{aligned}
\bar{E}_n(\rho_n) &= \frac{g_A^6 m_\pi^7}{(2\pi f_\pi)^6 u^3} \int_0^u dx \int_0^u dy\, \frac{x^3(u^2 - y^2)}{(1+4x^2)^2}(u-x)^2(2u+x) \\
&\quad \times \Bigg\{ xy(1 - 12x^2 + 4y^2) + 8x^3 \big[\arctan(2x+2y) - \arctan(2x-2y)\big] \\
&\quad + \Big(3x^4 - 2x^2 y^2 - y^4 - \frac{3x^2 + y^2}{2} - \frac{1}{16}\Big) \ln \frac{1+4(x+y)^2}{1+4(x-y)^2} \Bigg\}. \qquad (21)
\end{aligned}$$

The neutron density $\rho_n$ is related to the neutron Fermi momentum $k_n$ by $\rho_n = k_n^3/3\pi^2$. In eq.(21) and all following formulas for $\bar{E}_n(\rho_n)$ the dimensionless variable $u$ has the meaning $u = k_n/m_\pi$. Next one notices that for class I the right 2-ring diagram in Fig. 2 produces vanishing spin-trace.

Furthermore, one obtains from the U-type 1-ring diagram in Fig. 3 the following contributions:

$$\bar{E}(\rho) = \frac{g_A^6 m_\pi^7}{4(4\pi f_\pi)^6 u^3} \int_0^u dx \left\{ \Big[8G_S^2(x) + G_T^2(x)\Big] K_S(x) + \Big[8G_S(x) + G_T(x)\Big] G_T(x) K_T(x) \right\}, \qquad (22)$$

9

$$\bar{E}_n(\rho_n) = \frac{g_A^6 m_\pi^7}{12(4\pi f_\pi)^6 u^3} \int_0^u dx \left\{ \left[ 2G_S^2(x) + G_T^2(x) \right] K_S(x) + \left[ G_T(x) - 4G_S(x) \right] G_T(x) K_T(x) \right\}, \quad (23)$$

where we have introduced two new auxiliary functions:

$$K_S(x) = 2u - 3\arctan(u+x) - 3\arctan(u-x) + \frac{2 + u^2 - x^2}{2x} \ln \frac{1 + (u+x)^2}{1 + (u-x)^2}, \quad (24)$$

$$K_T(x) = \frac{u}{4x^2}(3 + 3u^2 - x^2) + \frac{1}{16x^3}\left[ x^2(x^2 + 2u^2 - 2) - 3(1 + u^2)^2 \right] \ln \frac{1 + (u+x)^2}{1 + (u-x)^2}, \quad (25)$$

defined by a tensorial Fermi sphere integral over a squared pion-propagator.

On the other hand the Z-type 1-ring diagrams give the following contributions:

$$\begin{aligned}
\bar{E}(\rho) &= \frac{g_A^6 m_\pi^7}{(4\pi f_\pi)^6 u^3} \int_0^u dx \int_0^u dy \left\{ 2G_S(x)G_S(y)\left[ \mathbf{D} - \mathbf{L} \right] + G_S(x)G_T(y) \right. \\
&\times \left[ 2\mathbf{D} - \frac{6x}{y} + \frac{\mathbf{L}}{2y^2}(3 + 3x^2 - y^2) \right] + G_T(x)G_T(y) \\
&\times \left. \left[ \frac{\mathbf{D}}{2} + \frac{3y}{8x} + \frac{27}{16xy} - \frac{\mathbf{L}}{64x^2y^2}(27 + 60y^2 + 2x^2y^2 + 6y^4) \right] \right\},
\end{aligned} \quad (26)$$

$$\begin{aligned}
\bar{E}_n(\rho_n) &= \frac{g_A^6 m_\pi^7}{6(4\pi f_\pi)^6 u^3} \int_0^u dx \int_0^u dy \left\{ G_S(x)G_S(y)\left[ \mathbf{D} - \mathbf{L} \right] + G_S(x)G_T(y) \right. \\
&\times \left[ \frac{6x}{y} - 2\mathbf{D} + \frac{\mathbf{L}}{2y^2}(y^2 - 3x^2 - 3) \right] + G_T(x)G_T(y) \\
&\times \left. \left[ \mathbf{D} + \frac{3y}{4x} + \frac{27}{8xy} - \frac{\mathbf{L}}{32x^2y^2}(27 + 60y^2 + 2x^2y^2 + 6y^4) \right] \right\},
\end{aligned} \quad (27)$$

with the rational function:

$$\mathbf{D} = \frac{1}{1 + (x-y)^2} - \frac{1}{1 + (x+y)^2}, \quad (28)$$

arising from an angular integral $\int_{-1}^1 dz \ldots$ over a squared pion-propagator.

Finally, the X-type 1-ring diagram leads to contributions of the form:

$$\begin{aligned}
\bar{E}(\rho) &= \frac{3g_A^6 m_\pi^7}{(4\pi f_\pi)^6 u^3} \int\limits_{|\vec{p}_j| < u} \frac{d^3 p_1\, d^3 p_2\, d^3 p_3}{(2\pi)^3} \frac{1}{(1 + \vec{q}_1^2)(1 + \vec{q}_2^2)} \\
&\times \left\{ 3\vec{q}_1^2\, \vec{q}_2^2 \left[ K_S(|\vec{\eta}|) - 2K_T(|\vec{\eta}|) \right] + (\vec{q}_1 \cdot \vec{q}_2)^2 \left[ 7K_T(|\vec{\eta}|) - K_S(|\vec{\eta}|) \right] \right. \\
&\left. + \frac{3}{\vec{\eta}^2} K_T(|\vec{\eta}|) \left[ 6\,\vec{q}_1^2\,(\vec{\eta} \cdot \vec{q}_2)^2 - 7(\vec{q}_1 \cdot \vec{q}_2)\,(\vec{\eta} \cdot \vec{q}_1)\,(\vec{\eta} \cdot \vec{q}_2) \right] \right\},
\end{aligned} \quad (29)$$

$$\begin{aligned}
\bar{E}_n(\rho_n) &= \frac{g_A^6 m_\pi^7}{(4\pi f_\pi)^6 u^3} \int\limits_{|\vec{p}_j| < u} \frac{d^3 p_1\, d^3 p_2\, d^3 p_3}{(2\pi)^3} \frac{1}{(1 + \vec{q}_1^2)(1 + \vec{q}_2^2)} \\
&\times \left\{ 3(\vec{q}_1 \cdot \vec{q}_2)^2 \left[ K_S(|\vec{\eta}|) + K_T(|\vec{\eta}|) \right] - \vec{q}_1^2\, \vec{q}_2^2 \left[ K_S(|\vec{\eta}|) + 2K_T(|\vec{\eta}|) \right] \right. \\
&\left. + \frac{3}{\vec{\eta}^2} K_T(|\vec{\eta}|) \left[ 2\,\vec{q}_1^2\,(\vec{\eta} \cdot \vec{q}_2)^2 - 3(\vec{q}_1 \cdot \vec{q}_2)\,(\vec{\eta} \cdot \vec{q}_1)\,(\vec{\eta} \cdot \vec{q}_2) \right] \right\},
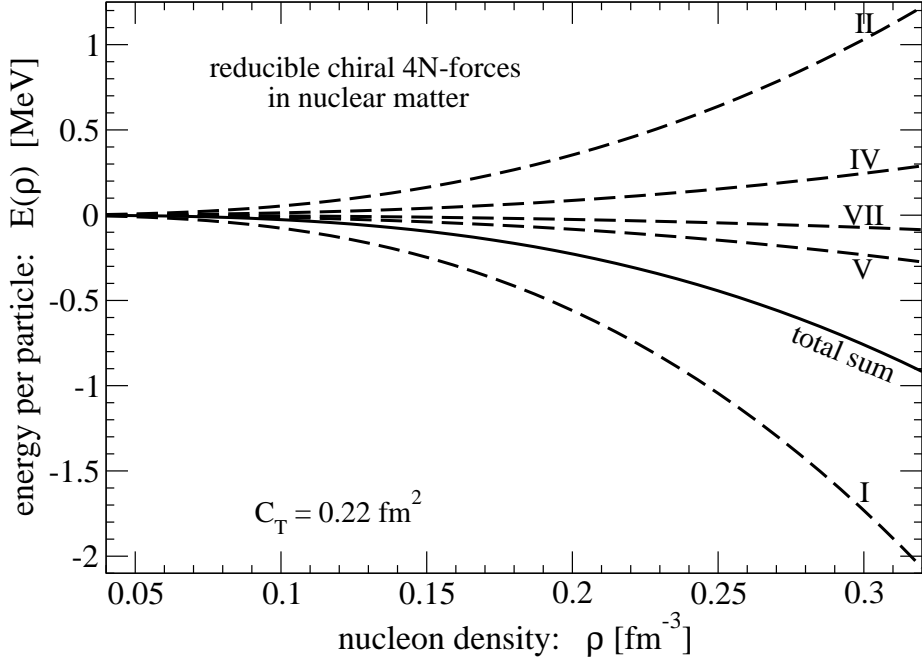\end{aligned} \quad (30)$$

Figure 4: Reducible chiral $4N$-interactions in isospin-symmetric nuclear matter. The dashed lines show the individual contributions from the five classes for $C_T = 0.22 \, \text{fm}^2$, and the full line gives their total sum.

with $\vec{q}_1 = \vec{p}_1 - \vec{p}_3$, $\vec{q}_2 = \vec{p}_2 - \vec{p}_3$ and $\vec{\eta} = \vec{p}_1 + \vec{p}_2 - \vec{p}_3$.

This completes our presentation of semi-analytical results for the energy per particle of isospin-symmetric nuclear matter $\bar{E}(\rho)$ and pure neutron matter $\bar{E}(\rho)$ as derived from the reducible chiral $4N$-interactions. The given formulas allow for an easy and accurate numerical evaluation [13] of these leading-order chiral four-body correlations.

# 3  Results and discussion

We are now in the position to present numerical results. The physical parameters related to pion-exchange are: $g_A = 1.29$ (nucleon axial-vector coupling constant), $f_\pi = 92.4 \, \text{MeV}$ (pion decay constant), and $m_\pi = 135 \, \text{MeV}$ (neutral pion mass). For the spin-spin contact-coupling $C_T$ we choose two opposite values, $C_T = 0.22 \, \text{fm}^2$ and $C_T = -0.45 \, \text{fm}^2$, taken from table I in ref.[9].

The contributions to the energy per particle $\bar{E}(\rho)$ of isospin-symmetric nuclear matter are presented in Fig. 4 for the small $C_T$-value, $C_T = 0.22 \, \text{fm}^2$, in the density region $\rho_0/4 < \rho < 2\rho_0$, with $\rho_0 = 0.16 \, \text{fm}^{-3}$ the empirical saturation density. The dashed lines (with appropriate labels) show separately the five classes (VII, V, IV, II, I) and the full line gives their total sum. One observes that class VII (proportional to $C_T^2$) is smallest in magnitude and that other classes (V+IV and II+I) cancel each other to a large extent. The largest repulsive and attractive contributions are provided by the $C_T$-independent classes II and I, respectively. As a consequence of these compensations the net attraction stays above $-1.3 \, \text{MeV}$ for all densities $\rho < 0.36 \, \text{fm}^{-3}$. The analogous results for the larger negative $C_T$-value, $C_T = -0.45 \, \text{fm}^2$, are shown in Fig. 5. One notices that class VII ($\sim C_T^2$) is still smallest in magnitude and that the classes V and IV have changed their position in comparison to the sequence in Fig. 4. The net attraction reaches now a value of $-1.7 \, \text{MeV}$ at $\rho = 0.36 \, \text{fm}^{-3}$. Exploring the whole range $|C_T| < 0.5 \, \text{fm}^2$ of the spin-spin contact-coupling $C_T$, one finds that the $4N$-attraction in nuclear matter does not exceed values of $-1.3 \, \text{MeV}$ for densities $\rho < 2\rho_0$.
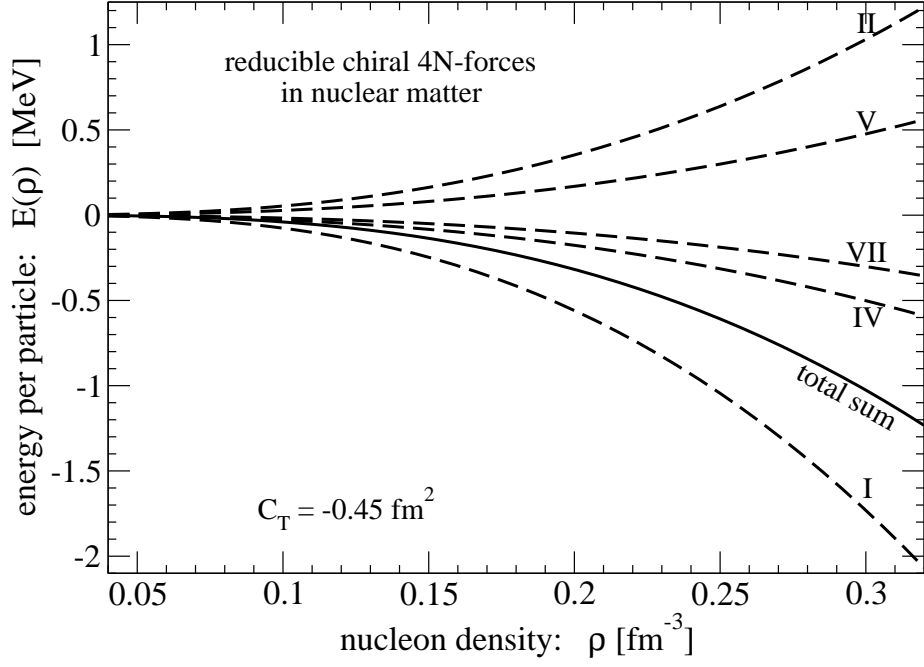
Figure 5: Reducible chiral $4N$-interactions in isospin-symmetric nuclear matter. The dashed lines show the individual contributions from the five classes for $C_T = -0.45\,\mathrm{fm}^2$, and the full line gives their total sum.

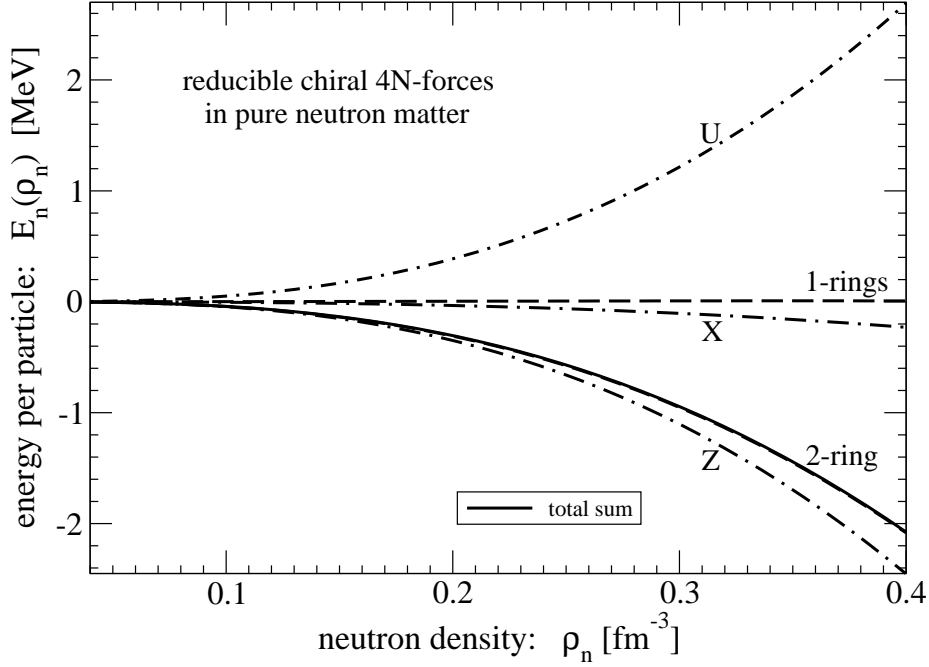

Figure 6: Reducible chiral $4N$-interactions in pure neutron matter. The conributions from 2-ring and 1-ring diagrams are shown separately. The U-type, Z-type, and X-type diagrams cancel each other almost completely.

In the case of pure neutron matter only class I (see subsection 2.5) contributes and the result for the energy per particle $\bar{E}_n(\rho_n)$ comes out parameterfree. Fig. 6 shows by the dashed lines the contributions from the 2-ring diagram and the sum of the three 1-ring diagrams in the density region $0.04\,\mathrm{fm}^{-3} < \rho_n < 0.4\,\mathrm{fm}^{-3}$. One recognizes that the latter part is extremely small. This feature has its origin in the almost complete compensation between the contributions from

12

the U-type, Z-type and X-type 1-ring diagrams, which are shown by the three dashed-dotted lines in Fig. 6. Interestingly, the net result for $\bar{E}_n(\rho_n)$ is thus entirely determined by the 2-ring part written in eq.(21). The corresponding attractive energy per particle goes approximately as $\rho_n^{7/3}$ and it reaches the value of about $-2.1\,\text{MeV}$ at the (relatively high) neutron density of $\rho_n = 0.4\,\text{fm}^{-3}$.

In passing we note that our numerical results for the chiral four-body correlations in nuclear and neutron matter agree perfectly [14] with those of the Darmstadt group [9] if the (unessential) regulator-function $f_R$ is set to $f_R = 1$.

In summary one can conclude that the chiral four-nucleon correlations studied in this work are at least one order of magnitude smaller than those provided by the strongly coupled $\pi N\Delta$-system [10] with its small mass-gap of $293\,\text{MeV} \simeq 1.1 k_{f0}$.

# Acknowledgements

# References

[1] E. Epelbaum, *Prog. Part. Nucl. Phys.* **57**, 654 (2006); and refs. therein.

[2] E. Epelbaum, H.-W. Hammer, Ulf-G. Meißner, *Rev. Mod. Phys.* **81**, 1773 (2009).

[3] S.K. Bogner, R.J. Furnstahl, A. Schwenk, *Prog. Part. Nucl. Phys.* **65**, 94 (2010).

[4] S.K. Bogner, R.J. Furnstahl, A. Nogga, A. Schwenk, *Nucl. Phys.* A **763**, 59 (2005).

[5] A. Nogga, S.K. Bogner, A. Schwenk, *Phys. Rev.* C**70**, 061002 (2004).

[6] K. Hebeler et al., *Phys. Rev.* C **83**, 031301 (2011).

[7] V. Bernard, E. Epelbaum, H. Krebs, Ulf-G. Meißner, *Phys. Rev.* C **77**, 064004 (2008).

[8] I. Tews, T. Krüger, K. Hebeler, A. Schwenk, *Phys. Rev. Lett.* **110**, 032504 (2013).

[9] T. Krüger, I. Tews, K. Hebeler, A. Schwenk, *Phys. Rev.* C bf 88, 025802 (2013).

[10] N. Kaiser, *Eur. Phys. J.* A **48**, 135 (2012).

[11] E. Epelbaum, *Phys. Lett.* B **639**, 456 (2006).

[12] E. Epelbaum, *Eur. Phys. J.* A **34**, 197 (2007).

[13] A Mathematica code can be obtained from the first author upon request.

[14] T. Krüger, TU Darmstadt, private communications.